

## Crystal growth and magnetic property of YFeO<sub>3</sub> crystal

ANHUA WU<sup>1,\*</sup>, HUI SHEN<sup>1,3</sup>, JUN XU<sup>1</sup>, ZHANLIANG WANG<sup>1</sup>, LINWEN JIANG<sup>1</sup>, LIQING LUO<sup>1</sup>, SHUJUAN YUAN<sup>2</sup>, SHIXUN CAO<sup>2</sup> and HUALJIN ZHANG<sup>4</sup>

<sup>1</sup>Shanghai Institute of Ceramics, Chinese Academy of Sciences, Shanghai 200050, China

<sup>2</sup>Department of Physics, Shanghai University, Shanghai 200444, China

<sup>3</sup>School of Materials Science and Engineering, Shanghai Institute of Technology, Shanghai 200235, China

<sup>4</sup>State Key Laboratory of Crystal Material, Shandong University, Jinan, 250100, China

MS received 8 March 2011; revised 4 May 2011

**Abstract.** YFeO<sub>3</sub> and other rare earth substituted crystals with distorted orthorhombic perovskite-like structure (space group, *Pbnm*) have attracted much attention due to their remarkable magnetic properties of primary significance for technological applications. In the present work, the floating zone growth of YFeO<sub>3</sub> crystals has been systematically investigated and high quality YFeO<sub>3</sub> crystal was obtained by optimized process. The magnetic properties of YFeO<sub>3</sub> crystal were investigated, and it indicated the high magneto-optical property in YFeO<sub>3</sub> crystals with specific orientation due to its anisotropy. YFeO<sub>3</sub> crystals display superior performance in the application magneto-optical current sensors and fast latching optical switches.

**Keywords.** Floating zone technique; single crystal growth; magnetic property.

### 1. Introduction

YFeO<sub>3</sub> and other rare earth substituted crystals with distorted orthorhombic perovskite-like structure (space group, *Pbnm*) have attracted much attention since 1950s due to their novel magnetic and magneto-optical properties, and are still the subject of much research aimed at a better understanding of properties of the magnetic subsystems and how interactions between them depend on external parameters (Bozorth *et al* 1956, 1958; Treves 1962; Bazaliy *et al* 2004).

Along with fundamental property measurements, research into possible device applications of orthoferrites has also been undertaken by many groups in the 1960s and 1970s (Bobeck *et al* 1969; Laudise 1972). The interest in orthoferrites took off in the 1990s, since they have been overtaken by ferromagnetic garnets for magnetic bubble devices. However, their highest domain wall motion velocity (at up to 20 km/s) is reported to be the highest known in any magnetically ordered media (Demokritov *et al* 1991; Didosyan 1994). Recent investigations by Didosyan and co-workers report that orthoferrites show promising use in various innovative micro-technological devices, such as fast latching type optical switches, light spot position measurements, magneto-optical current sensors and magnetic field sensors (Didosyan and Hauser 2000; Didosyan *et al* 2002, 2004). More recently, laser-induced ultrafast spin reorientation was found in TmFeO<sub>3</sub>, DyFeO<sub>3</sub> and HoFeO<sub>3</sub> crystals, which may have far-reaching influence on emerging spintronic devices (Kimel *et al* 2004, 2005, 2009).

These potential applications have created a high demand for availability of sizable and high quality RFeO<sub>3</sub> crystals. So far, single crystal YFeO<sub>3</sub> has been grown by several methods. Flux method was most often used (Remeika 1956; Wanklyn 1969; Giess *et al* 1970; Quon and Potvin 1971). It is apparent from the literature that flux grown orthoferrite crystals invariably suffer from inclusions, second phase formation including oxyfluorides, garnet and PbFe<sub>12</sub>O<sub>19</sub> and other defects, while only relatively small crystals have been obtained. Many attempted growths employing both the Czochralski method and slow cooling techniques yielded only small, defective crystals with inclusions high in Fe<sup>2+</sup> (Barilo *et al* 1991). Voids, bubbles, twins and optical density variations are commonly observed in crystals grown by hydrothermal and seeded Bridgman methods (Blank *et al* 1971; Kolb and Laudise 1971; Nielsen and Blank 1972). All above mentioned methods have difficulties in growing high quality YFeO<sub>3</sub> crystals.

The floating zone crystal growth method with an infrared convergence type heater can easily reach a high temperature exceeding the melting point of YFeO<sub>3</sub> crystal and can avoid the contamination because no crucible is needed and a moderate temperature gradient is realized (Fairholme *et al* 1971; Balbashov and Egorov 1981; Koohpayeh *et al* 2007). In the present work, the floating zone growth of YFeO<sub>3</sub> crystals has been systematically investigated and high quality YFeO<sub>3</sub> crystal was obtained by seeded growth through optimized process. Meanwhile the magnetic measurements of YFeO<sub>3</sub> crystal were carried out using a superconducting quantum interference device magnetometer (Quantum design, PPMS-9).

\*Author for correspondence (wuanhua@mail.sic.ac.cn)

## 2. Experimental

The starting materials for the preparation of feed rods for the floating zone crystal growth were  $Y_2O_3$  (99.99%) and  $Fe_2O_3$  (99.99%) powders. Stoichiometric amounts of the raw materials of absolute ethanol for 24 h were milled in the present study. After drying and screening, the mixture was calcined at  $1100^\circ C$  for 20 h in air with an intermediate grinding to improve its homogeneity. After confirmation by X-ray diffraction that the constituents had converted to the orthoferrite structure, the powder was packed and subsequently sealed into a rubber tube while being evacuated using a vacuum pump. The powder was then compacted into a rod, typically 6 mm in diameter and 80 mm long, using a hydraulic press under an isostatic pressure of 100 MPa. After removal from the rubber tube, the rods were sintered in a vertical tube furnace at  $1600^\circ C$  for 8 h in air.

The growth apparatus used was an image furnace with double ellipsoidal mirrors (NEC Machinery SC-N35HD-L), in which two-halogen lamps of 1.5 kW were used as a heat source. Disk-shaped samples were cut directly from the cross-sections of the crystals using a diamond wheel, which were cut from selected crystals. The magnetic measurements were carried out using a PPMS-9.

## 3. Results and discussion

### 3.1 Float zone growth of yttrium orthoferrite single crystals

Single crystals were grown from the feed rods in a double ellipsoidal mirror optical floating zone furnace having  $2 \times 1.5$  kW halogen lamps as the heating source. An initial unseeded run was performed to produce a crystal that was used as a seed for all subsequent growths. The feed rod was suspended at the upper shaft and the seed rod was attached to the lower shaft. Both the feed rod and seed rod moved downwards and the melting zone was formed. The feed and seed shafts rotated at 5–20 rpm in opposite directions and the crystal was grown from the bottom to top in a vertical direction. The traveling rate of the melting zone was in the range of 2.5–7.5 mm/h in 1 bar of oxygen. Several seed crystals were grown by spontaneous nucleation through feed rod passing molten zone, which was as shown in figure 1. Koohpayeh indicated that erbium orthoferrite single crystal was inclined to grow along  $\langle 391 \rangle$  orientation along its length (Koohpayeh *et al* 2007). In our earlier study, various orientated crystals were obtained by spontaneous nucleation, and each one had a small angle included from the b direction. A  $\langle 120 \rangle$ -orientated seed was obtained by selecting from these crystals (Shen *et al* 2007).

Seed growth of  $YFeO_3$  crystal is similar to the spontaneous nucleation, only  $\langle 120 \rangle$ -orientated seed was attached to the lower shaft instead of seed rod. Based on the experiment of the crystal growth by spontaneous nucleation, the optimized growth parameters were confirmed. During all of



**Figure 1.**  $YFeO_3$  crystal grown by spontaneous nucleation with FZ method.



**Figure 2.**  $YFeO_3$  crystal grown by seeded FZ method.

the growths, the growth process was realized by simultaneous downward movement of both feed rod and seed crystal, crystallization was completed through feed rod passing the molten zone induced by seed crystal. There is a necking process at the beginning of crystal growth to ensure the crystal strictly grew along the orientation of the seed crystal. During the necking process, travel rate of feed rod was manually adjusted based on the crystallization situation while the travel rate of seed crystal was 5 mm/h. After the necking process was completed, both the travel rate of seed crystal and feed rod was 5 mm/h. Growths were carried out under 1 bar oxygen, with rotation rates of 30 rpm for the growing crystal or seed crystal (lower shaft) and 5 rpm for feed rod (upper shaft) during whole growth process. In all runs, only one zone pass was performed.

Crystals were grown at growth rates of 5 mm/h; a typical as-grown  $YFeO_3$  boule obtained using the image furnace is shown in figure 2. X-ray Laue analysis showed all of the crystals have adopted the  $\langle 120 \rangle$ -orientation of the seed crystal. One apparent difference between seeded-growth crystals and the crystals grown by the spontaneous nucleation, which could be clearly seen by the naked eye, was that the

surfaces of the seeded-growth crystals produced were shiny and smooth, whereas the spontaneous nucleation gave crystals with a rough and non-uniform surface. The compositional homogeneities, crystalline qualities, inclusion defects, second phases and surface morphology have been investigated on the  $\text{YFeO}_3$  crystals grown by the spontaneous nucleation systematically, which was shown in the paper by Shen *et al* (2007).

### 3.2 Magnetic measurements

As noted previously,  $\text{YFeO}_3$  is a canted antiferromagnet meaning that the atomic moments align at an angle to the  $c$ -axis such that the components of magnetization perpendicular to the  $c$ -axis cancel out, whereas the components of atomic magnetization parallel to the  $c$ -axis give a spontaneous magnetization in the  $c$ -axis. Disk-shaped sample was cut directly from the cross-section of the crystals which grows along  $\langle 120 \rangle$ - orientation. In the previous work,

we obtained (100) wafer from the  $\text{YFeO}_3$  crystals grown by spontaneous nucleation. The magnetization vs magnetic field ( $M$ - $H$ ) curve of  $\text{YFeO}_3$  single crystal was measured in the (100) wafer and (120) wafer at room temperature, respectively, which was shown in figure 3.

No matter whether it is (100) wafer or (120) wafer, the magnetic field is perpendicular to the  $c$ -axis when the magnetization is normal to the plane of  $\text{YFeO}_3$  crystal. Whereas magnetic field is parallel to or have an angle to  $c$ -axis when the magnetization is parallel to the plane of  $\text{YFeO}_3$  crystal. The saturation magnetization ( $M_s$ ) is 0.81 emu/g and 1.53 emu/g for (100) wafer and (120) wafer, respectively while the magnetic field is perpendicular to the  $c$ -axis. In comparison, the  $M_s$  is 0.18 emu/g and 0.039 emu/g for (100) wafer and (120) wafer, respectively while magnetic field is parallel to the plane of  $\text{YFeO}_3$  crystal. The huge difference in the saturation magnetization can be attributed to the antiferromagnetic structure, in which the components of magnetization perpendicular to the  $c$ -axis is cancelled out

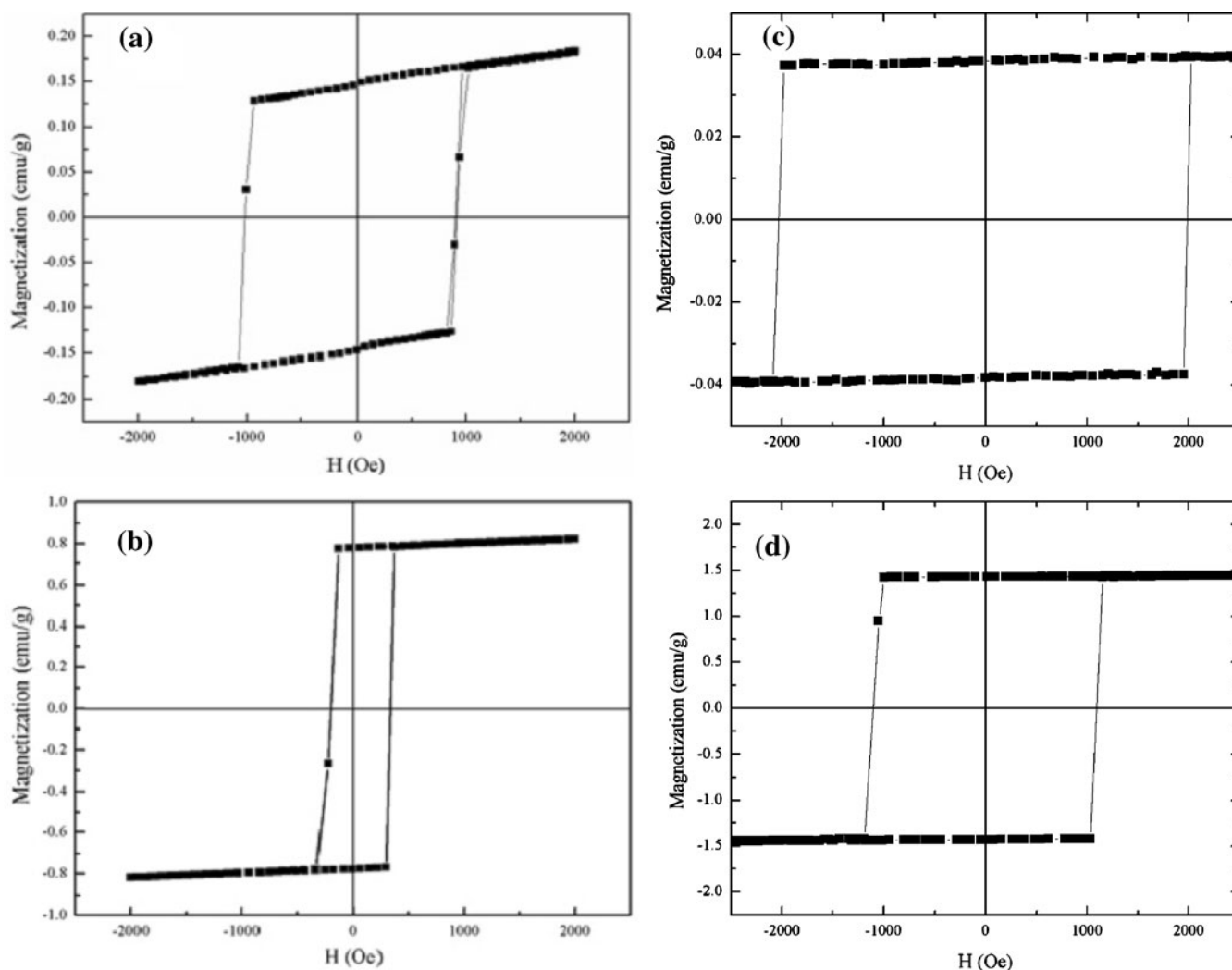


**Figure 3.** The  $M$ - $H$  curve for the magnetization parallel and normal to the plane of  $\text{YFeO}_3$  crystal. (a) parallel to (100), (b) normal to (100), (c) parallel to (120) and (d) normal to (120).

due to the atomic moments of adjacent  $\text{Fe}^{3+}$  aligned at an angle to the  $c$ -axis. For the (120) wafer, the coercive  $H_c$  is about 1990 Oe and 1020 Oe when the magnetization is parallel and normal to the plane of  $\text{YFeO}_3$  crystal. However, it is only 970 Oe and 260 Oe for (100) wafer which is obtained from the  $\text{YFeO}_3$  crystals grown by the spontaneous nucleation. The investigation on  $\text{ErFeO}_3$  crystal indicated that the crystal which contained second phase inclusions will have very narrow hysteresis loop due to the second phase inclusions acting as nucleation site for domain reversal; whereas, the crystal free from second phase inclusions will have a significantly wider loop (Koochpayeh *et al* 2007). In this work, the wide hysteresis loop of (120) sample proved that the high quality  $\text{YFeO}_3$  crystals have been grown by the seeded FZ method.

Rare-earth orthoferrites ( $\text{RFeO}_3$ , where R is a rare-earth ion) is a canted antiferromagnet, exhibiting ferromagnetic behaviour. A characteristic feature of  $\text{RFeO}_3$  is the presence of two magnetic subsystems of  $\text{R}^{3+}$  and  $\text{Fe}^{3+}$ . The competition of Fe–Fe, R–Fe and R–R interactions leads to a few interesting phenomena in these materials. The corresponding spin arrangement is a canted antiferromagnetic structure with a small total ferromagnetic moment directed along the  $c$ ( $c//z$ ) crystal axis, and an antiferromagnetic vector directed along the  $a$  ( $a//x$ ) crystal axis. The rare-earth ions remain paramagnetic but develop a magnetic moment in the molecular field of the iron ions subsystem (Tsymbal *et al* 2005). Thus the saturation magnetization displays large difference when the magnetic field is parallel and normal to the plane of  $\text{YFeO}_3$  crystal. The high quality  $\text{YFeO}_3$  crystal is grown by the seeded FZ method free from second phase inclusions, it displays larger difference in perpendicular and parallel saturation magnetization than the spontaneous nucleation grown crystal.

The zero-field-cooled (ZFC) magnetization along the (120) of the single crystal were measured in the temperature range from 2 to 350 K under an applied field of 2000 Oe. As shown in figure 4, the magnetization decreases with increase in temperature and this is the difference from  $\text{HoFeO}_3$  and other  $\text{RFeO}_3$  crystal. The magnetization increases abruptly with increase in temperature between 50 K and 58 K along the  $c$ -axis, but decreases abruptly along the  $a$ -axis in  $\text{HoFeO}_3$  crystal (Shao *et al* 2011). The abrupt change of ZFC in  $\text{HoFeO}_3$  and other  $\text{RFeO}_3$  crystal is attributed to spin reorientation transition due to  $4f$  electrons in  $\text{R}^{3+}$  ions. The special characteristic of ZFC in  $\text{YFeO}_3$  crystal is original from  $\text{Y}^{3+}$  special outside ionic structure of ( $3d^0$ ).

The curve displays obvious rectangular hysteretic loop, thus only a small coil is needed for switching when  $\text{YFeO}_3$  crystal was used as a rotator for magneto-optical switch. There is no need of an external magnetic field for providing stable states of the rotator, which substantially reduces the switching time thanks to its rectangular hysteretic loop. In addition, the  $\text{YFeO}_3$  crystal can be saturated by applying a smaller magnetic field of even lower than 1000 Oe in some specifically given orientation, while a larger magnetic field (1780 Oe) is needed to saturate  $\text{Y}_3\text{Fe}_5\text{O}_{12}$  (YIG) crystal.

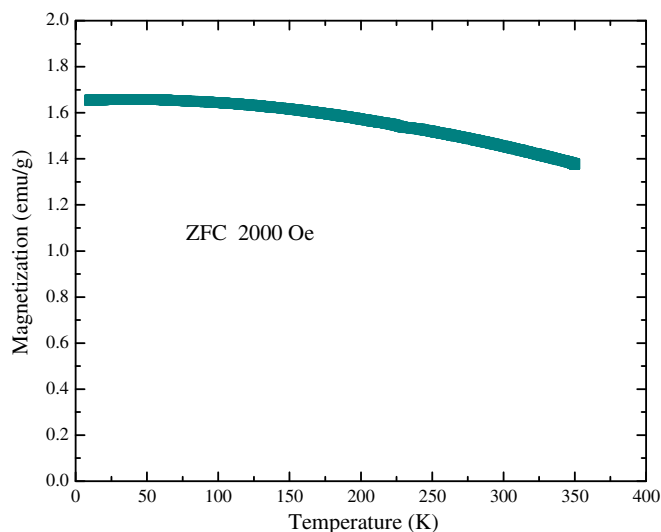


**Figure 4.** Temperature dependence of magnetization after ZFC along (120) in  $\text{YFeO}_3$  crystal measured at 2000 Oe.

A magneto-optical rotator saturated by lower external magnetic field is desired to produce a more compact isolator with a smaller magnet. Accordingly, smaller electric current is needed for the coils to get the desired magnetic field. The heat generated during the operation is lessened, improving the temperature stability and lifetime of the devices (Shen *et al* 2009).

#### 4. Summary and perspective

High quality yttrium orthoferrite single crystals were grown by seeded floating-zone growth method. Magnetic measurements on  $\text{YFeO}_3$  crystals indicated the high magneto-optical property in  $\text{YFeO}_3$  crystals with specific orientation due to its anisotropy.  $\text{YFeO}_3$  crystals display superior performance in application of magneto-optical current sensors and fast latching optical switches due to its rectangular hysteretic loop and small saturation magnetic field in specific orientation. Meanwhile, the axis of weak ferromagnetism of  $\text{YFeO}_3$  crystal is the crystallographic  $c$  axis, thus it is the key task to obtain  $\langle 001 \rangle$ -orientation seed crystal and realize crystal growth along  $c$  axis for the crystal growth and investigation will be carried out systematically on magnetic property of  $\text{YFeO}_3$  crystal in the future.

#### Acknowledgements

The authors would like to acknowledge the financial support from the National Natural Science Foundations of China (Grant No. are 50932003 and 51002097). This work is also supported by the Opening Project of State Key laboratory of Crystal Material (Grant No. KF1006) and the Shanghai Municipal Education commission (No.11YZ223)

## References

- Balbashov A M and Egorov S K 1981 *J. Cryst. Growth* **52** 498
- Barilo S N, Ges A P, Guretskii S A, Zhigunov D I, Ignatenko A A, Luginets A M and Shapovalova E F 1991 *J. Cryst. Growth* **108** 309
- Bazaliy Y B, Tsymbal L T, Nakazei G N and Wigen P E 2004 *J. Appl. Phys.* **95** 6622
- Blank S L, Shick L K and Nielsen J W 1971 *J. Appl. Phys.* **42** 1556
- Bobeck A H, Fischer R F, Perneski A J, Remeika J P and Van Uitert L G 1969 *IEEE Trans. Magn. Mag.* **5** 544
- Bozorth R M, Williams H J and Walsh D E 1956 *Phys. Rev.* **103** 572
- Bozorth R M, Kramer V and Remeika J P 1958 *Phys. Rev. Lett.* **1** 3
- Demokritov S O, Kirilyuk A I, Kreines N M, Kudinov V I, Smirnov V B and Chetkin M V 1991 *J. Magn. Magn. Mater.* **102** 339
- Didosyan Y S 1994 *J. Magn. Magn. Mater.* **133** 425
- Didosyan Y S and Hauser H 2000 *IEEE Trans. Instr. Meas.* **49** 14
- Didosyan Y S, Hauser H, Fiala W, Nicolics J and Toriser W 2002 *J. Appl. Phys.* **91** 7000
- Didosyan Y S, Hauser H, Raider G A and Toriser W 2004 *J. Appl. Phys.* **95** 7339
- Fairholme R J, Gill G P and Marsh A 1971 *Mater. Res. Bull.* **6** 1131
- Giess E A, Crinemeyer D C, Rosier L L and Kuptsis J D 1970 *Mater. Res. Bull.* **5** 495
- Kimel A V, Kirilyuk A, Tsvetkov A, Pisarev R V and Rasing T 2004 *Nature* **429** 850
- Kimel A V, Kirilyuk A, Usachev P A, Pisarev R V, Balbashov A M and Rasing T 2005 *Nature* **435** 655
- Kimel A V, Ivanov B A, Pisarev R V, Usachev P A, Kirilyuk A and Rasing T 2009 *Nature Phys.* **5** 1369
- Kolb E D and Laudise R A 1971 *J. Appl. Phys.* **42** 1552
- Koohpayeh S M, Abell J S, Bamzail K K, Bevan A I, Fort D and Williams A J 2007 *J. Magn. Magn. Mater.* **309** 119
- Laudise R A 1972 *J. Cryst. Growth* **13/14** 27
- Nielsen J W and Blank S L 1972 *J. Cryst. Growth* **13/14** 702
- Quon H H and Potvin A J 1971 *J. Cryst. Growth* **10** 124
- Remeika J P 1956 *J. Am. Ceram. Soc.* **78** 4259
- Shao M, Cao S, Wang Y, Yuan S, Kang B, Zhang J, Wu A and Xu J 2011 *J. Cryst. Growth* **318** 947
- Shen H, Xu J, Wu A, Yu J, Liu Y and Luo L 2007 *Cryst. Res. Technol.* **42** 943
- Shen H, Xu J, Wu A, Zhao J and Shi M 2009 *Mater. Sci. Eng.* **B157** 77
- Treves T 1962 *Phys. Rev.* **125** 1843
- Tsymbal L T, Kamenev V I, Bazaliy Y B, Khara D A and Wigen P E 2005 *Phys. Rev.* **B72** 52413
- Wanklyn B M 1969 *J. Cryst. Growth* **5** 323